



## Numerical modelling and structural analysis of a 1 MW tidal turbine blade

Title	Numerical modelling and structural analysis of a 1 MW tidal turbine blade
Author(s)	Jiang, Yadong;Finnegan, William;Wallace, Finlay;Flanagan, Michael;Flanagan, Tomas;Goggins, Jamie
Publication Date	2022-01-31
Publisher	MARINE 2021
Repository DOI	<a href="https://doi.org/10.2218/marine2021.6799">https://doi.org/10.2218/marine2021.6799</a>

# Structural Analysis of a 1 MW Tidal Turbine Blade through Full-Scale Physical Testing and a Digital Twin

MARINE 2021

Yadong Jiang<sup>1,2\*</sup>, William Finnegan<sup>1</sup>, Finlay Wallace<sup>3</sup>, Michael Flanagan<sup>2</sup>, Tomas Flanagan<sup>2</sup> and Jamie Goggins<sup>1</sup>

<sup>1</sup> SFI MaREI Centre for Energy, Climate and Marine, Ryan Institute & School of Engineering, National University of Ireland, Galway, Ireland (NUIG), University Road, H91 TK33 Galway, Ireland. Email: yadong.jiang@nuigalway.ie, william.finnegan@nuigalway.ie, jamie.goggins@nuigalway.ie, web: <https://www.nuigalway.ie/structures>

<sup>2</sup> ÉireComposites Teo, An Choill Rua, Inverin, H91 Y923 Galway, Ireland. Email: y.jiang@eirecomposites.com, m.flanagan@eirecomposites.com, t.flanagan@eirecomposites.com, web: <https://www.eirecomposites.com>

<sup>3</sup> Orbital Marine Power, Innovation Centre – Orkney, Hatston Pier Road Kirkwall, Orkney, Scotland, KW15 1ZL, UK. Email: f.wallace@orbitalmarine.com, web: <https://www.orbitalmarine.com>

\* Corresponding author: Yadong Jiang, yadong.jiang@nuigalway.ie

## ABSTRACT

This paper presents a study of the structural response of a rotor blade that was designed for a 1 MW floating tidal turbine device. The 8 m long blade was manufactured by ÉireComposites Teo and its structural performance was experimentally evaluated under mechanical loading in the Large Structures Research Laboratory at National University of Ireland Galway (NUIG). The FE model of the rotor blade was developed based on layered shell elements. A digital twin of the rotor blade was developed and validated in this paper. In effect, the digital twin is a finite element model (FEM) generated in ANSYS. By simulating the blade response under the design loads using the digital twin, a difference of 3% is found in the blade tip deflection between the physically measured test results in the laboratory and numerical prediction from the digital twin. The results not only guarantee that the blade can withstand the maximum design loads, but also demonstrate good accuracy of the digital twin.

**Keywords:** Tidal Turbine; Ocean Energy; Turbine Rotor Blade; Digital Twin; Experimental Testing; Marine Engineering.

## 1. INTRODUCTION

As one of the main alternatives to fossil fuels, renewable energy is developing rapidly in recent decades. In 2019, renewable energy contributes about 10% of global total primary energy demand (IEA 2020). As regulated by the moon, the tidal stream is almost 100% predictable, making it a reliable renewable energy resource. Despite the multiple countrywide lock-downs due to COVID-19, the cumulative tidal stream technology deployed in Europe is 27.9 MW in 2020, making up 77% of the global total tidal energy device installations (OEE 2021). In 2030, the predicted tidal energy devices deployed in Europe are 1,324 MW and 2,388 MW under the low growth and high growth scenarios, respectively (OEE 2020). Recently, several

projects (MeyGen<sup>1</sup>, SABELLA<sup>2</sup>, FloTEC<sup>3</sup>, etc.) were carried out to accelerate the development and commercialisation of tidal energy conversion devices. However, the development of tidal turbines still remains at an early stage compared to wind turbines, due to commercial confidentiality and lack of available test results. As tidal turbines convert ocean current to kinetic energy through rotor rotating, the structural performance of tidal turbine blades is of main concern. Since the water density is 835 times higher than that of air, tidal turbine blades suffer from complex loading. Hence, there are significant challenges regarding the design and performance validation of a tidal turbine blade. The static testing can ensure blade safety under extreme tidal loading conditions.

For predicting the stiffness, strength and fatigue life, finite-element (FE) analysis is commonly performed in the structural design of tidal turbine blades. For modelling wind turbine blades, the layered shell elements are usually used (Wang *et al.* 2016, Fagan *et al.* 2017, Fagan *et al.* 2018, Peeters *et al.* 2019). Since the structure of tidal turbine blades is similar to that of wind turbine blades, this modelling methodology was also utilised to design the tidal turbine blades (Murray *et al.* 2016, Fagan *et al.* 2016, Jiang *et al.* 2019, Fagan *et al.* 2019). However, due to a lack of available testing results, the accuracy and efficiency of the developed FE model were not validated against experimental data. This paper presents the structural behaviour study of a 1 MW tidal turbine blade, one of the largest turbine in the world, based on experimental testing and numerical analysis. The blade structural details are illustrated. The testing programme, including the natural frequency tests and the static tests, are detailed. The FE model developed for predicting the structural response of the blade is proposed. The blade performance under the design loads and the accuracy of the FE model is studied based on the test and numerical results.

## 2. METHODOLOGY

### 2.1 Blade Description

The 8 m tidal turbine rotor blade tested in the study was designed for a floating tidal energy conversion device of Orbital Marine Power (OMP). The device contains two 1 MW tidal turbines, each with a rotor diameter of 20 m. The tidal blade consists of the main body, the trailing edge fairings and the tip. Figure 1 shows the main body of the tidal turbine blade. It was manufactured by ÉireComposites using glass fibre reinforced powder epoxy composite material, based on the ÉireComposites' Composites Powder Epoxy Technology (CPET). In comparison to the conventional glass fibre reinforced polymer (GFRP), the GFRP manufactured based on CPET has certain advantages, including small through-thickness wet out requirement, good fibre volume fraction control and low exotherm during cure. Regarding the raw material, different from the traditional epoxy resins, the power epoxy can be stored at ambient temperatures and has a long shelf life. The material properties used in the manufacturing are listed in Table 1, which is supplied by the manufacturer.

The blade trailing edge fairings and the tip are to be manufactured separately to the main body. Since the two components are to optimise the hydrodynamic shape of the blade, they are considered not to contribute significantly to resisting the primary hydrodynamic loads. Therefore, the trailing edge fairings and the tip are not included in the structural tests. The main body of the blade was manufactured in two stages. In the first stage, the upper half, the lower half and the web of the blade were built separately using CPET. In this stage, the three components were not fully cured. In the second stage, the three components were bonded together, using prepregs as the connection elements. The main body was fully cured under high temperature in this stage.

---

<sup>1</sup> MeyGen | Tidal Projects, SIMEC Atlantis Energy. <http://simecatlantis.com/projects/meygen/>, accessed 04/2021.

<sup>2</sup> SABELLA's tidal turbines: tidal stream power to trigger the energy transition. <https://www.sabella.bzh/en/>, accessed 04/2021.

<sup>3</sup> FloTEC: Innovation and Networks Executive Agency - European Commission. <https://ec.europa.eu/inea/en/horizon-2020/projects/h2020-energy/ocean/flotec>, accessed 04/2021.



**Figure 1.** The main body of the tidal turbine blade (manufactured at ÉireComposites).

**Table 1.** Material properties.

	UD	BX	unit
Density	1900	1900	kg/m <sup>3</sup>
E <sub>1</sub>	38805	25944	MPa
E <sub>2</sub>	12785	25944	MPa
E <sub>3</sub>	12785	25944	MPa
G <sub>12</sub>	3670	3570	MPa
G <sub>13</sub>	3670	3570	MPa
G <sub>23</sub>	3670	3570	MPa
v <sub>12</sub>	0.26	0.1289	-
v <sub>13</sub>	0.26	0.1289	-
v <sub>23</sub>	0.26	0.1289	-

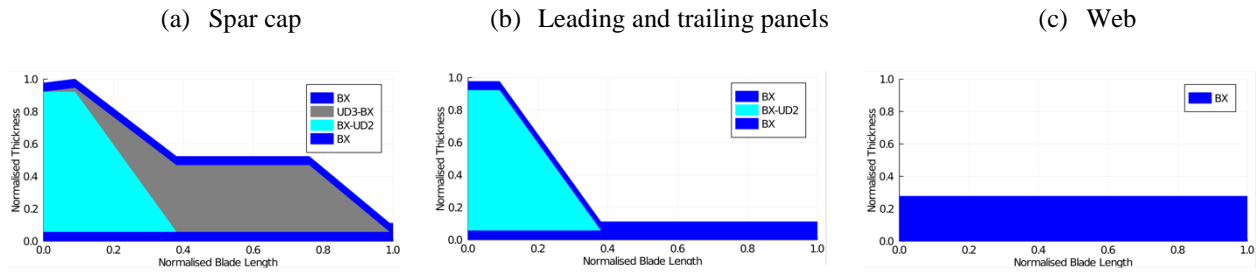
According to the structural details supplied by the manufacturer, the blade external surface can be divided into three components, namely the spar cap, the leading panel and the trailing panel. There is one web inside the main body, ranging from circa 1 m from the root up to the tip. The web connects the upper and lower spar caps to form an I-beam, working as the main support component of the blade. The blade layer thickness distributions are shown in The UD presents a layer with a number of uni-directional laminates.

The BX presents a layer with a number of woven laminates.

The UD3-BX presents a layer constructed by 25% of woven laminates and 75% of uni-directional laminates.

The BX-UD2 presents a layer constructed by 33.3% of woven laminates and 66.7% of uni-directional laminates.

Figure 2, where the thickness values are normalised by the maximum thickness. The UD presents a layer with a number of uni-directional laminates. The BX presents a layer with a number of woven laminates. The UD3-BX presents a layer with a laminate with 25% of woven laminates and 75% of uni-directional laminates. The BX-UD2 presents a layer with a laminate with 33.3% of woven laminates and 66.7% of uni-directional laminates. The blade root cross-section is designed to be circular and is connected to the turbine pitch bearing via 48 steel inserts. The root region is the strongest of the blade as it should withstand the moments generated from the tidal stream. Compared to the leading and trailing panels, the spar cap has an extra BX-UD3 layer in between the external and internal covers to increase its resistance against the flapwise loads. It should be noted that only with the GFRP material used, the shell of this tidal turbine blade is thick enough to avoid the local buckling failure. Hence, different from a typical wind turbine blade, there is no light-wight in-fill materials used in the blade to increase the shell thickness.



The UD presents a layer with a number of uni-directional laminates.  
 The BX presents a layer with a number of woven laminates.  
 The UD3-BX presents a layer constructed by 25% of woven laminates and 75% of uni-directional laminates.  
 The BX-UD2 presents a layer constructed by 33.3% of woven laminates and 66.7% of uni-directional laminates.

**Figure 2.** Summary of the layup details of the tidal turbine blade.

## 2.2 Experimental Testing

A series of tests, aiming to study the structural performance of the tidal turbine blade, were carried out at the Large Structures Testing Laboratory at NUI Galway. In this paper, the natural frequency tests and the static tests are detailed. As can be seen in Figure 3, the blade main body was mounted to a root support frame, which was designed to withstand the loads expected during the static testing. The blade main body was mounted to the support frame at a pitch angle of  $6^\circ$  through 48 steel inserts, with its pressure side facing the upward direction. The support frame was fixed to the reinforced concrete reaction floor.

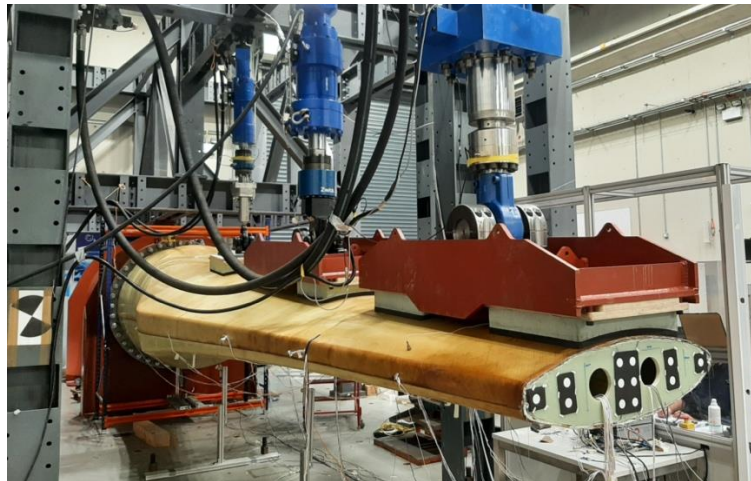


**Figure 3.** Blade test setup.

Natural frequency tests were performed to determine the dynamic properties of the blade. In these tests, 5 and 3 single-axis accelerometers were installed along the pressure side and the leading edge, respectively, to record the blade vibration responses. To excite the blade, a hammer was used to introduce a transient impact to the tip. The first two flapwise and edgewise modes, as well as the first torsional mode, are of interest. To obtain the flapwise and torsional modes, the transient impact was imposed in the flapwise direction, while for the edgewise mode, the edgewise impact was imposed. The natural frequencies of the blade were acquired based on Fast Fourier transform (FFT) analyses. Each type of test was repeated 3 times and the average values were used.

The static testing aims to ensure that the tidal turbine rotor blade can withstand the design load cases. The tests were carried out based on the DNVGL-ST-0164 code (DNV, 2015) and the IEC TS 61400-23 standards (IEC, 2014). To distribute the design loads along the blade length, the testing loads were applied by three servo-hydraulic actuators (Figure 3). The actuators (called actuator 1, 2 and 3) were mounted to the reaction frame

with distances of 3.28 m, 5.13 m and 7.19 m to the blade root. The load applied from actuator 1 was directly distributed to the blade surface through a contact pad. Regarding the actuators 2 and 3, the steel load introduction devices were used to split the loads equally. As can be seen in Figure 3, each device was connected to the actuator through a swivel and could split the applied load into two contact pads. By using this load introduction mechanism, the testing loads were distributed to 5 contact areas on the blade. This ensures an accurate representation of the design loads.

There were 8 load cases, with loads increasing up to the maximum loads, considered in the static tests. The loads applied in each test are listed in Table 2. It should be noted that the loads were applied in the downward direction and the blade was installed in a pitch angle of 6°. Therefore, the loads applied by the actuators can be decomposed in flapwise and edgewise directions. As the edgewise extreme loads are not considered to be critical for the blade design, the actuators loads were calibrated so that the flapwise design loads were fitted. Under the calibrated loads, about 50% of the edgewise design loads were achieved. Torsional extreme loads are not considered to be critical for the blade design, and hence, were not included in the test campaign.

**Table 2.** Static load cases and the corresponding actuator loads.

	<b>Actuator 1 [kN]</b>	<b>Actuator 2 [kN]</b>	<b>Actuator 3 [kN]</b>
<b>Load Case 12.5%</b>	19	61	45
<b>Load Case 25%</b>	39	123	90
<b>Load Case 37.5%</b>	58	184	135
<b>Load Case 50%</b>	78	245	180
<b>Load Case 62.5%</b>	97	306	225
<b>Load Case 75%</b>	116	368	270
<b>Load Case 87.5%</b>	136	429	315
<b>Load Case 100%</b>	155	490	360

To monitor the response of the blade under different load cases, strain gauges and displacement transducers were installed. The displacement transducers, namely the linear variable differential transformers (LVDT, linearity 0.1%) and linear potentiometers (linearity 0.1%) were installed at the locations 3.28 m, 5.13 m and 7.94 (from the root) to measure the blade deflections. At 6 cross-sections (0.5 m, 2.16 m, 3.96 m, 5.13 m, 6.16 m and 7.19 m from the root), the electrical resistance strain gauges (gauge factor uncertainty, 1%) were installed at different locations to monitor the strain development on the blade surface. Figure 4 displays the typical strain gauge locations at each cross-section. Additionally, there are LVDTs and strain gauges installed on the support frame to monitor the blade root rotation and to ensure that the frame does not fail ahead of the blade.

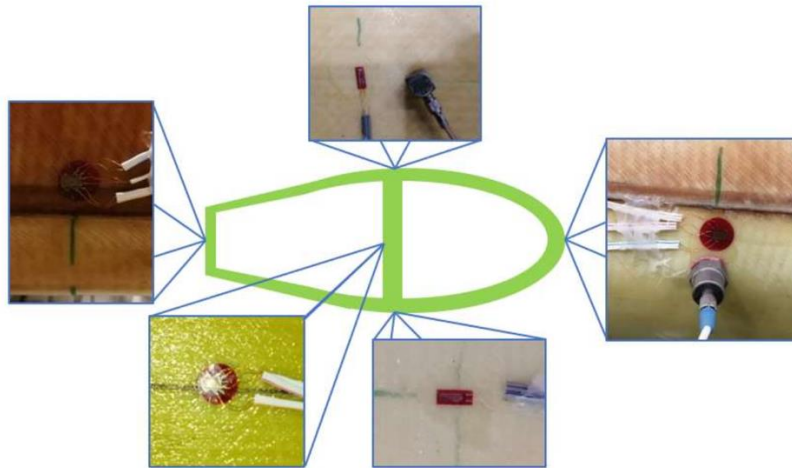


**Figure 4.** Typical instrumentation at a cross section of the blade, including linear and rosette electrical resistance strain gauges (linear gauges top and bottom photos; rosette gauges left and bottom-left photos) and accelerometers (top and right photos).

### 2.3 Numerical Modelling

The finite-element (FE) model of the tidal turbine blade was generated in software Ansys® Academic Research Mechanical, Release 17.1 (ANSYS, 2016). Similar to a typical FE model of the wind turbine blade, the blade model is constructed with shell element SHELL181, which contains 4 nodes with six degrees of freedom at each node. For each shell element, layered shell sections with multiple layers (3 integration points per layer) are assigned. **Error! Reference source not found.** shows the meshed FE model generated for simulating the static tests. The mesh nodes which were supposed to be in contact with the pads were selected, as highlighted in **Error! Reference source not found.**. The loads applied to each contacting pad were calculated and these loads were uniformly distributed to the selected nodes. It should be noted that, for simplifying the model, the connections between the upper half, lower half and the web are assumed to be strong enough for the resisting the loads. Hence, the connection detail are neglected and the blade is modelled as an integrated part.

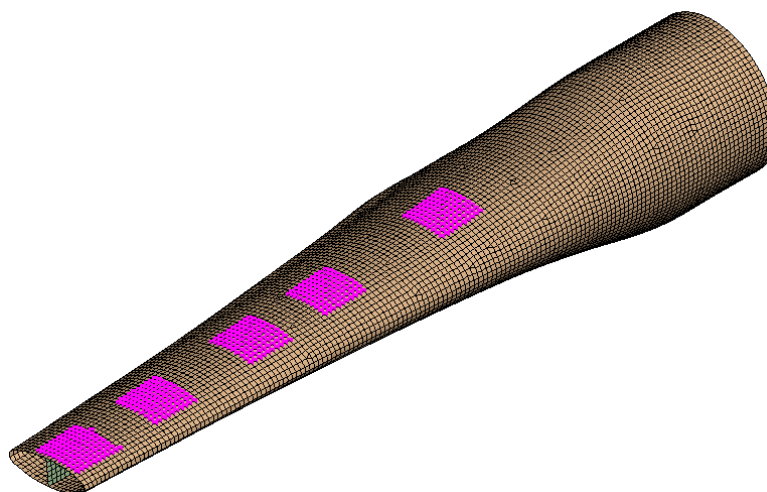


**Figure 5.** FE model generated in Ansys® Academic Research Mechanical, Release 17.1 (ANSYS, 2016).

## 3. RESULTS AND DISCUSSION

### 3.1 Natural Frequencies

Table 3 summarises the natural frequency values obtained from testing and predicted by the FE model. The numerical results do not have good agreements with the test data. The first three predicted frequencies are more than 40% higher than the test results, while the predicted first torsional frequency is 15% less than the test value. Additionally, the second edgewise mode was not captured by the FE analysis. The inaccurate numerical values could result from two reasons. Firstly, the weight of the FE model is 3,820 kg, while the total weight of the blade is over 4,000 kg. The 48 steel inserts and the additional prepreg materials, used for connecting the blade halves and the web, were neglected in the FE model. Therefore, the predicted blade mass is less than the real data. Secondly, the values listed in the table represent the natural frequencies of the whole testing system. The support frame could add flexibilities to the system and leads to the inaccurate prediction of the natural frequency values.

**Table 3.** Natural frequencies from the test and from the FE analysis.

<b>Mode</b>	<b>Test Frequency [Hz]</b>	<b>FE Frequency [Hz]</b>
<b>1st Flapwise</b>	15.28	21.99
<b>1st Edgewise</b>	17.81	26.36
<b>2nd Flapwise</b>	31.34	54.79
<b>2nd Edgewise</b>	31.48	NA
<b>1st Torsional</b>	84.51	71.66

### 3.2 Static Testing

With the increasing of the loads in the 8 load cases, the blade main body behaved consistently. Hence, four load cases, namely 25%, 50%, 75% and 100% of design load cases, were selected for results discussion and FE analysis, to reduce congestion in displaying the results. Under the maximum design load (100% load case), no failure or cracks were observed, demonstrating that the blade has the structural integrity to withstand the design loads. Under the static loading, the blade root slightly rotated under the large root moment (5714 kNm). This root rotation was obtained by the displacement data provided by a pair of LVDTs installed at the support frame. Under the 100% load case, the blade had a root rotation of  $0.17^\circ$ . Considering that the blade is about 8 m long, this rotation resulted in an additional deflection of circa 23 mm at the tip. Hence, the deflection values recorded by the three displacement transducers were corrected with the root rotation angle. Figure 6 summarises the blade deflections under the four load cases. The maximum blade tip deflection is 104 mm, 1.3% of the blade length, proving that the tidal turbine blade has good stiffness.

The predicted blade deflections from the digital twin are compared with the test data in Figure 6. In the four load cases, the numerical results from the digital twin have a very good agreement with the experimental data. Under the 100% design load, the predicted tip deflection was about 101 mm, 3% less than the value obtained from the physical laboratory test. Hence, the FE model could predict the stiffness of the tidal turbine rotor blade accurately. It can be observed that the FE analysis slightly underestimates the deflections for the four load cases, indicating that the stiffness of the model is marginally higher than that suggested by the physical laboratory tests.

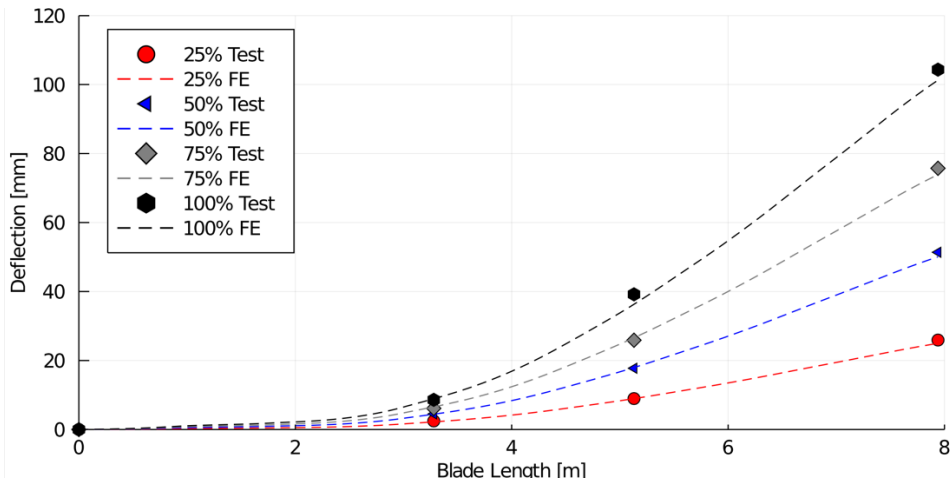


**Figure 6.** Deflection comparisons between the testing data and FE results.

The normalised longitudinal direction strain along the spar cap, the leading and trailing edges of the selected four load cases are plotted along the length of the blade in Figure 7, where the strain are normalised based on the maximum absolute values. The longitudinal direction is defined as the direction from the root to the tip. The maximum absolute strain, 0.002, occurred on the pressure side of the spar cap, under the 100% load case. Considering that the strain limit of the BX GFRP is about  $\pm 0.025$ , it indicates that no material failure under the maximum design loads. The strain data predicted by the FE analysis are plotted and compared with the test data in Figure 7. For strain values, along the spar caps on the pressure side and suction side, the FE-predicted strain has good agreements with that from the strain gauges. Overall, the predicted values are marginally lower than the test data. It indicates that the FE model has slightly overestimated the blade stiffness, which is in line with the observations from the deflection comparisons. However, there is a large difference between the numerical and experimental strain results along the leading and trailing edges. This difference can result from the connection details. As mentioned in section 2.1, the upper and lower halves of the blade main body were connected along the leading and trailing edges, using the prepregs, which were not considered in the numerical modelling. The simplification of connection details can lead to inaccurate strain prediction in the numerical analysis. This observation is in line with the conclusions made by Peeters *et al.* (2019), where the authors pointed out the shell element wind turbine FE model could predict the deflection well, but failed in simulating the stress/strain distribution at the connection region.

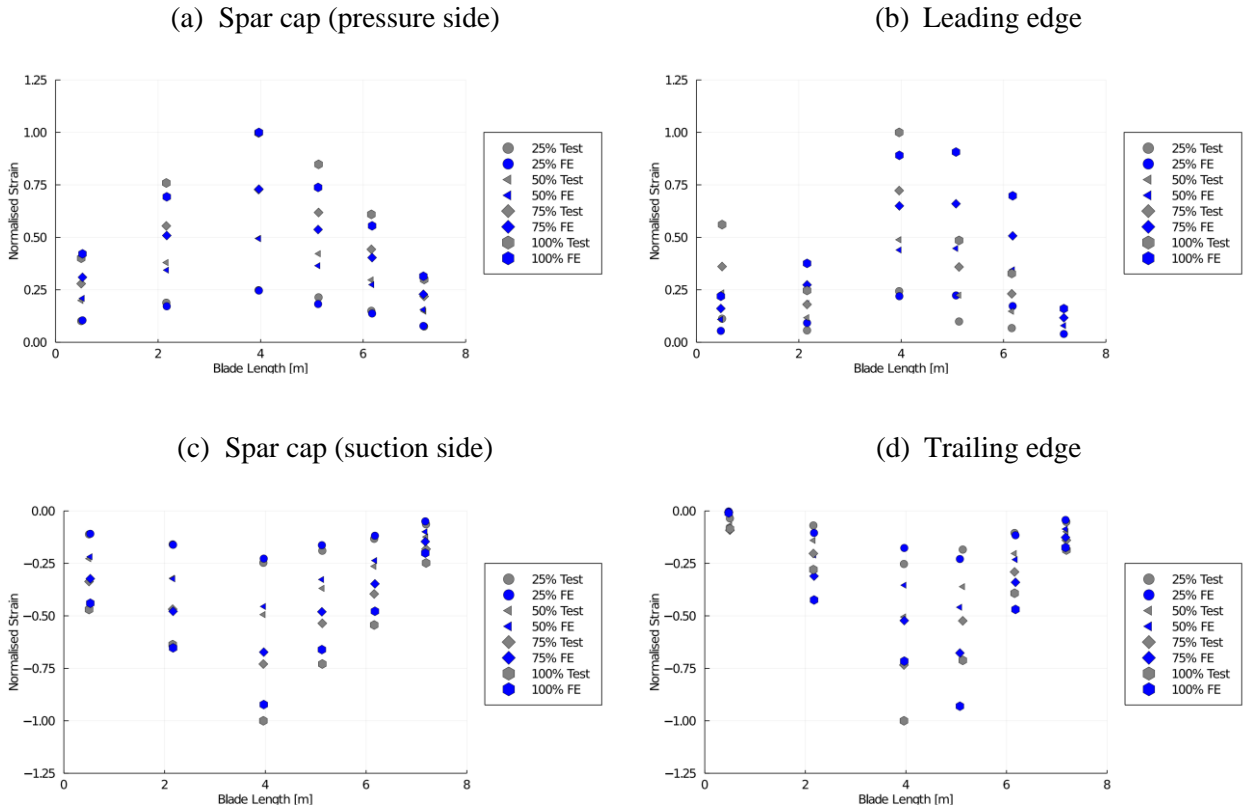


**Figure 7.** Normalised longitudinal direction strain comparisons along the length of the blade between the testing data and FE results.

#### 4. CONCLUSIONS

In this paper, a series of experimental tests were carried out to study the structural behaviour of a 1 MW tidal turbine rotor blade. According to the blade design details and the testing programme, an FE model, constructed based on layered shell elements, was developed for the tidal turbine rotor blade. Based on the results from the physical testing and digital twin, the performances of the blade under the design loads, as well as the accuracy of the FE model, were discussed. The following conclusions are proposed:

- By performing static testing, the tidal turbine blade was proved to withstand the maximum design loads. No failure or cracks were observed during testing, which ensures blade safety under extreme load conditions as it has the required strength.
- The developed shell element model that formed the digital twin can give an accurate prediction of the blade deflection under testing loads. Moreover, the strain values on the spar cap can also be accurately predicted, indicating that the shell element is suitable for modelling tidal turbine blades as the spar caps are the main load carrying structure of the blade.
- However, with the simplification of connection details, the digital twin failed to closely predict the natural frequencies and the strain data along the leading and trailing edges.

In the future, the connection details of the blade will be considered in the FE modelling. Based on the stress and strain output from the numerical results, fatigue analysis will be carried out to guarantee the blade's 20-year operation life.

## ACKNOWLEDGEMENTS

This work is funded by the Sustainable Energy Authority of Ireland (SEAI) through Ocean ERA- NET 2018 SEABLADE project (Grant no. 18/OCN/102), the European Commission H2020 ‘Marine Renewable Infrastructure Network for Enhancing Technologies 2 (MARINET 2)’ programme (Grant no. 26255) and the H2020 FloTEC project (Grant no. 691916). The research is also the support by Science Foundation Ireland (SFI) through MaREI Research Centre for Energy, Climate and Marine (Grant no. 12/RC/2302\_2). The first author would like to acknowledge the support of SFI through the SFI Industry Fellowship Programme (Grant no. 19/IFA/7417).

## REFERENCES

- Ansys® Academic Research Mechanical, Release 17.1 Help System. (2016). *Mechanical Application Documentation*, ANSYS, Inc.
- DNV. (2015). *Standard DNVGL-ST-0164 Tidal turbines*. Det Norske Veritas (2015).
- Fagan, E.M., Kennedy, C.R., Leen, S.B. and Goggins, J. (2016). Damage mechanics based design methodology for tidal current turbine composite blades. *Renewable Energy*, 97, 358-372.
- Fagan, E.M., Flanagan, M., Leen, S.B., Doyle, A. and Goggins, J. (2017). Physical experimental static testing and structural design optimisation for a composite wind turbine blade. *Composite Structures*, 164, 90-103.
- Fagan, E.M., De La Torre, O., Leen, S.B. and Goggins, J. (2018) Validation of the multi-objective structural optimisation of a composite wind turbine blade. *Composite Structures*, 204, 567-577.
- Fagan, E.M., Wallace, F., Jiang, Y., Kazemi, A. and Goggins, J. (2019). Design and testing of a full-scale 2 MW tidal turbine blade. *Proceedings of the Thirteenth European Wave and Tidal Energy Conference*, Napoli, Italy.
- IEA. (2020). *World Energy Outlook 2020*. International Energy Agency, Paris, France.
- IEC. (2014). *IEC 61400 - 23: 2014: Wind turbine generator systems—part 23: full - scale structural testing of rotor blades*. International Electrotechnical Commission, Geneva, Switzerland.
- Jiang, Y., Fagan, E.M. and Goggins, J. (2019). Structural design and optimisation of a full-scale tidal turbine blade. *Proceedings of the Thirteenth European Wave and Tidal Energy Conference*, Napoli, Italy.
- Murray, R.E., Nevalainen, T., Gracie-Orr, K., Doman, D. and Pegg, M.J. (2016). Passively adaptive tidal turbine blades: Design tool development and initial verification. *International Journal of Marine Energy*, 14, 101-124.
- OEE. (2021). *Ocean Energy - Key trends and statistics 2020*. Ocean Energy Europe, Brussels, Belgium.
- OEE. (2020). *2030 Ocean Energy Vision*. Ocean Energy Europe, Brussels, Belgium.
- Peeters, M., Santo, G., Degroote, J. and Van, P.W (2019). Comparison of Shell and Solid Finite Element Models for the Static Certification Tests of a 43 m Wind Turbine Blade. *Energies*, 11, 1346.
- Wang, L., Kolios, A., Nishino, T., Delafin, P. and Bird, T. (2016). Structural optimisation of vertical-axis wind turbine composite blades based on finite element analysis and genetic algorithm. *Composite Structures*, 153, 123-138.